A Performance Analysis of OFDM Systems in Excessively Dispersive Multipath Channels

Wookwon Lee and Christopher S. Curry

Abstract: **For orthogonal frequency division multiplexing (OFDM), the discrete Fourier transform (DFT)-based processing at the receiver has been perceived equivalent to the matched filter (MF)-based processing. In this paper, we revisit the equivalence and mathematically show that when the guard interval is insufficient, the well-known DFT-based processing inherently causes more intersymbol and interchannel interference (ISI/ICI) than the MF-based processing. Then, with the adverse increase of interference, analytical expressions for the link performance are derived in terms of bit error rate (BER). Numerical results from computer simulation and analysis are presented to justify our claims.**

Index Terms: **Discrete Fourier transform (DFT), dispersive multipath channel, interchannel interference (ICI), intersymbol interference (ISI), orthogonal frequency division multiplexing (OFDM).**

I. INTRODUCTION

For the signal processing in orthogonal frequency division multiplexing (OFDM) systems, the inverse discrete Fourier transform (IDFT) at the transmitter is well known to be equivalent to the traditional subcarrier modulation with an array of oscillators [1]. Correspondingly, the discrete Fourier transform (DFT)-based and the matched filter (MF)-based processing at the receiver have been perceived equivalent, regardless of whether the maximum channel delay, $\tau_{\max}$, exceeds the guard interval (GI), T_g, or not. The equivalence indeed holds when $\tau_{\max} \leq T_g$ as initially shown in [1].

Interestingly, however, our preliminary experiment reveals that for the same OFDM parameters and in a common multipath channel with $\tau_{\max} > T_g$, the mathematical expressions of these two processing models do not produce the same numerical values at the output of their OFDM demodulator, i.e., DFT or MF. Also from computer simulation, it is observed that they are equivalent only when the MF-based processing is performed with N samples per OFDM block while the simulation data do not agree with the numerical data from its mathematical expression. Moreover, when the MF-based processing is simulated with more samples, i.e., an integer multiple of N samples per OFDM block, its MF output values tend to approach those from analytical expressions.

Motivated by these observations, in this paper, we revisit the mathematical equivalence of the DFT-/MF-based processing in [2] and [3] with emphasis on the multipath channel with $\tau_{\max} > T_g$. To the authors' knowledge, the equivalence has never been proven when the GI is insufficient. The study on the intersymbol/interchannel interference (ISI/ICI) caused by multipath channels when $\tau_{\max} > T_g$ might be arguable but is indeed important for a complete understanding of OFDM, as evident from the previous research [4]–[6]. The contributions of this paper are i) to analytically show that at the receiver the equivalence holds only for multipath channels with $\tau_{\max} \leq T_g$ but not for $\tau_{\max} > T_g$, ii) to demonstrate that the DFT-based processing causes more ISI/ICI than the MF-based when $\tau_{\max} > T_g$, and iii) to provide accurate analytical expressions of bit error rates (BERs) taking into account the difference in ISI/ICI. For the BER evaluation, among various results in the literature [7]–[9], we extend the analysis in [8].

The rest of this paper is organized as follows. In Section II, we briefly revisit the MF-/DFT-based processing at the receiver to better understand the origin of discrepancy between the two models and in Section III, exact mathematical expressions are provided along with illustrative examples for the discrepancy. Analytical expressions and numerical results are presented in Section IV for the effect of discrepancy on the link performance and finally, conclusions are made in Section V.

II. TWO MODELS OF OFDM PROCESSING

A. MF-Based Processing

Consider an OFDM communication system where complex data signals are serial-to-parallel converted and de-multiplexed onto a set of N orthogonal continuous-time subcarriers with an appropriate guard interval inserted. For the continuous-time baseband signal at the receiver, a bank of MFs are employed for coherent demodulation. Then, adopting the notations in [2], the time-domain transmitted signal for a stream of OFDM blocks can be written as

$$x(t) = \sum_{n=-\infty}^{+\infty} \sum_{k=0}^{N-1} X_{n,k} \phi_k (t - nT_b') \tag{1}$$

where $\{X_{n,k}\}$ are the complex baseband data for the n-th OFDM block, T_b' is the OFDM block duration equal to the sum of the guard interval T_g and the effective block duration T_b. The orthogonal basis functions $\{\phi_k(t)\}$ are defined as $\phi_k(t) = e^{j2\pi f_k t}$ with the k-th subcarrier frequency $f_k \triangleq f_c + k/T_b$ and f_c the fundamental frequency. The orthogonal basis functions are primarily defined over T_b but also assumed to maintain mutual orthogonality over T_b'. For notational simplicity but without loss of generality, we assume that f_c is zero and the noise at the receiver is omitted until Section IV.

For the multipath channel, a finite impulse response (FIR) function $h(t)$ is assumed for N_p path components such that

Manuscript received August 31, 2005; approved for publication by Daesik Hong, Division II Editor, May 10, 2006.

W. Lee is with the Department of Electrical Engineering, University of Arkansas, Fayetteville, AR 72701 USA, email: wookwon@uark.edu.

C. S. Curry was with the Department of Electrical Engineering, University of Arkansas, Fayetteville, AR 72701 USA. He is now with the Raytheon Co., Dallas, TX 75234 USA, email: christopher_s_curry@raytheon.com.

$h(t) = \sum_{l=0}^{N_p-1} h_l(t)\delta(t-\tau_l)$ where $h_l(t) \triangleq a_l e^{j(\theta_l+2\pi f_{D_l}t)}$ is a normalized complex path gain with a_l, θ_l, and f_{D_l} denoting the real path gain, phase variation, and Doppler frequency, and τ_l is the relative delay of the l-th path. We consider that the maximum path delay $\tau_{\max} = \tau_{N_p-1}$ can be longer than the GI but shorter than the effective OFDM block duration, i.e., $\tau_{\max} < T_b$, and the Doppler shift is relatively small such that $f_D T_b' \ll 1$.

In the receiving end, following a similar approach in [2], we can write the k-th MF output, $Y_{n,k}$, for a multipath channel with some (but not all) path delays exceeding the GI as

$$\begin{aligned} Y_{n,k} &= \sum_{l\in\{\tau_l\leqslant T_g\}} h_{l,n}e^{-j2\pi f_k\tau_l}X_{n,k} + \sum_{l\in\{\tau_l>T_g\}} h_{l,n}\mu_{k,k}(\tau_l)X_{n,k} \\ &\quad + \sum_{l\in\{\tau_l>T_g\}}\sum_{\substack{m=0\\m\neq k}}^{N-1} h_{l,n}\mu_{m,k}(\tau_l)X_{n,m} \\ &\quad + \sum_{l\in\{\tau_l>T_g\}}\sum_{m=0}^{N-1} h_{l,n}\lambda_{m,k}(\tau_l)X_{n-1,m} \end{aligned} \tag{2}$$

where the third and fourth terms are the overall ICI and ISI, respectively, $h_{l,n} \triangleq h_l(nT_b')$, and

$$\mu_{m,k}(\tau_l) = \begin{cases} \frac{T_b-\tau_l+T_g}{T_b}e^{-j2\pi f_m\tau_l}, & \text{if } m=k \\ \frac{T_g-\tau_l}{T_b}e^{-j[2\pi f_m\tau_l-\pi(f_m-f_k)(\tau_l-T_g)]} \\ \times \operatorname{sinc}(\pi(f_m-f_k)(\tau_l-T_g)), & \text{otherwise} \end{cases} \tag{3}$$

$$\lambda_{m,k}(\tau_l) = \begin{cases} \frac{\tau_l-T_g}{T_b}e^{-j2\pi f_m(\tau_l-T_b')}, & \text{if } m=k \\ \frac{\tau_l-T_g}{T_b}e^{-j[2\pi f_m(\tau_l-T_b')-\pi(f_m-f_k)(\tau_l-T_g)]} \\ \times \operatorname{sinc}(\pi(f_m-f_k)(\tau_l-T_g)), & \text{otherwise} \end{cases} \tag{4}$$

which are dependent upon τ_l, T_g, and T_b in particular.

B. DFT-Based Processing

For the same OFDM system as in Section II-A but in a form of discrete-time signals processed with the N-point IDFT/DFT, let L denote the length of GI normalized to the fundamental period, $T \triangleq T_b/N$, of OFDM. For the channel impulse response $h(t)$, the path delay τ_l can be rounded to an integral multiple of T with the normalized channel length of L_c, i.e., $\tau_{\max} = (L_c-1)T$. The complex path gain c_m at $t = mT$ is given by h_l if $m = \lfloor \tau_l/T \rfloor$; otherwise 0, for $m = 0, \cdots, L_c-1$. Then, after the DFT operation, the frequency-domain received signal $\mathbf{Y}_n$, which corresponds to $\{Y_{n,k}\}$ in (2), can be written as

$$\mathbf{Y}_n = \frac{1}{N}\mathbf{W}_N\left(\tilde{\mathbf{C}}_{n-1}\mathbf{W}_N^c\mathbf{X}_{n-1} + \tilde{\mathbf{C}}_n\mathbf{W}_N^c\mathbf{X}_n\right) \tag{5}$$

where $\mathbf{W}_N$ is the N-dimensional DFT matrix, $\mathbf{X}_n$ is an $N\times 1$ vector of complex baseband data, the superscript $(\cdot)^c$ denotes the complex conjugate, and $\tilde{\mathbf{C}}_i$ for $i \in \{n-1, n\}$ is a modified subchannel matrix of size $(N\times N)$ given in [3].

III. DISCREPANCY IN MF-/DFT-BASED PROCESSING

In deriving the expression (2) or (5), the MF operation, i.e., *integrate and sample* over T_b, or the DFT operation for the current OFDM block is straightforward when $\tau_l \leqslant T_g$ as the previous OFDM block signals do not appear in the integration interval and the basis functions maintain mutual orthogonality over that duration. But when $\tau_l > T_g$, the previous block signals do appear in the integration interval and thus, mutual orthogonality is destroyed among all subcarriers and ISI terms, i e., $\lambda_{m,k}(\tau_l)X_{n-1,m}$ for all m, and ICI terms, i.e., $\mu_{m,k}(\tau_l)X_{n,m}$ for $m \neq k$, appear as shown in (2). This is well known for OFDM, either with the MF- or DFT-based processing. However, as will be shown below, when $\tau_l > T_g$, the degree of non-orthogonality between a received subcarrier signal and other basis functions turns out to be different between the MF- and DFT-based processing, and this difference results in a different level of ISI/ICI between them, destroying their equivalence.

Below, as the MF-based processing is typically implemented in a discrete-time format, we first convert the expression in (2) by properly replacing the continuous-time parameters with discrete-time ones and compare it with (5). Although our focus is on the case of $L_c - 1 > L$ but for the purpose of comparison, the case of $L_c - 1 \leqslant L$ is also presented.

A. Maximum Path Delay $L_c - 1 \leqslant L$

For a discrete-time form of (2), let k and m represent the subcarrier and time indices, respectively, normalized to the fundamental period T, i.e., k/N from $f_k = k/T_b = k/NT$ and m from $t = mT$. The path gains are normalized to the total power gain of 1. Then, for $L_c - 1 \leqslant L$, with only the first summation remaining, (2) becomes

$$Y_{n,k} = \sum_{m=0}^{L_c-1} c_m e^{-j2\pi mk/N}X_{n,k}. \tag{6}$$

For (5), it can be easily verified that $\tilde{\mathbf{C}}_{n-1} = \mathbf{0}_N$ and the DFT output is simplified to

$$\mathbf{Y}_n = \mathbf{H}_N^{(n)}\mathbf{X}_n \tag{7}$$

where $\mathbf{H}_N^{(n)} \triangleq (1/N)\mathbf{W}_N\tilde{\mathbf{C}}_n\mathbf{W}_N^c$ is an N-dimensional diagonal matrix with its diagonal element $H_{kk} = \sum_{m=0}^{L_c-1} c_m \cdot e^{-j2\pi mk/N}$, which is the well-known DFT-ed channel impulse response for the subcarrier k. From (6) and (7), it is clear that there is no mathematical discrepancy in the MF- and DFT-based processing when $L_c - 1 \leqslant L$.

B. Maximum Path Delay $L_c - 1 > L$

In this case, with $T_b = NT$, $T_g = L$, and $T_b' = (N+L)T$, and the MF and DFT outputs given by (2) and (5), respectively, can be collectively written as

$$\mathbf{Y}_n = [\mathbf{H}_N^{(n-1)}\ \mathbf{H}_N^{(n)}]\begin{bmatrix}\mathbf{X}_{n-1}\\ \mathbf{X}_n\end{bmatrix} \tag{8}$$

where $\mathbf{H}_N^{(i)} \triangleq (1/N)\mathbf{W}_N\tilde{\mathbf{C}}_i\mathbf{W}_N^c$ with its kp-th elements of

$$H_{kp}^{(n)} = \begin{cases} \sum_{m\in\{m\leqslant L\}} c_m e^{-j2\pi mk/N} + \sum_{m\in\{m>L\}} c_m \mu_{kk}(m), & \text{if } p = k \\ \sum_{m\in\{m>L\}} c_m \mu_{kp}(m), & \text{if } p \neq k \end{cases} \tag{9}$$

$$H_{kp}^{(n-1)} = \sum_{m\in\{m>L\}} c_m \lambda_{kp}(m) \tag{10}$$

where

$$\lambda_{kp}(m) \triangleq \begin{cases} \frac{(m-L)}{N} e^{-j2\pi p(m-(N+L))/N}, & \text{if } p = k \\ \frac{\beta_{kp}(m,L)}{N} e^{-j2\pi p(m-(N+L))/N}, & \text{if } p \neq k \end{cases} \tag{11}$$

$$\mu_{kp}(m) \triangleq \begin{cases} \frac{(N-m+L)}{N} e^{-j2\pi km/N}, & \text{if } p = k \\ -\frac{\beta_{kp}(m,L)}{N} e^{-j2\pi pm/N}, & \text{if } p \neq k \end{cases} \tag{12}$$

with

$$\beta_{kp}(m,L) = \begin{cases} \sum_{\ell=0}^{m-(L+1)} e^{-j2\pi\ell(k-p)/N} & \text{for DFT} \\ e^{j\pi(p-k)(m-L)/N}(m-L) & \\ \quad \times \operatorname{sinc}\left(\frac{\pi(p-k)(m-L)}{N}\right) & \text{for MF} \end{cases} \tag{13}$$

which is herein referred to as the *discrepancy factor* (DF). Note that in $\mathbf{H}_N^{(i)}$ for both $i = n$ and $n-1$, the main diagonal elements given by (9) and (10) for $p = k$ are the same for the DFT- and MF-based processing as $\lambda_{kp}(m)$ and $\mu_{kp}(m)$ are not affected by $\beta_{kp}(m, L)$, but off-diagonal elements, i.e., $p \neq k$, are not the same since $\lambda_{kp}(m)$ and $\mu_{kp}(m)$ are scaled by $\beta_{kp}(m, L)$, which is different in the DFT-/MF-based processing. This translates into a different level of total ISI/ICI.

C. Numerical Examples

An illustrative example of the DF, $\beta_{kp}(m, L)$, is shown for subcarrier $k = 1$ in Fig. 1 where the DF is evaluated at $m = 18$ and 19 with $N = 64$, $L = 16$, and $L_c - 1 = 20$. Note that the discrepancy is relatively small when the distance between k and p is small, e.g., up to $p = 35$ in Fig. 1(a) and $p = 45$ in Fig. 1(b), but as the distance further increases, the discrepancy rapidly increases as the DF for the DFT-based processing increases. Moreover, the maximum value of the DF for the DFT-based processing depends on the maximum path delay as its value is accumulated as shown in (13).

The discrepancy can be further illustrated by comparing data from simulation and numerical evaluation at the OFDM demodulator output. For brevity but without compromising its meaning and interpretation of the data, we use a small N such that $N = 8$, $L = 4$, and $T_b' = 4.0$ μs. The power delay profile (PDP) of the multipath channel is assumed to be exponentially decaying and modeled with $p_{\text{ch}}(m) = e^{-m/m_{\text{df}}}$ where m_{df} determines how slowly the PDP decays with time and is assumed to be 50. Furthermore, only two paths are assumed to be non-zero while $m \in \{0, L_c - 1\}$ with $L_c \in \{5, 6\}$ such that the case of $L_c - 1 \leqslant L$ is illustrated with $L_c = 5$ and the case of $L_c - 1 > L$ with $L_c = 6$. A stream of complex data $\{X_{n,k}\} \in \{-1, 1\}$ for

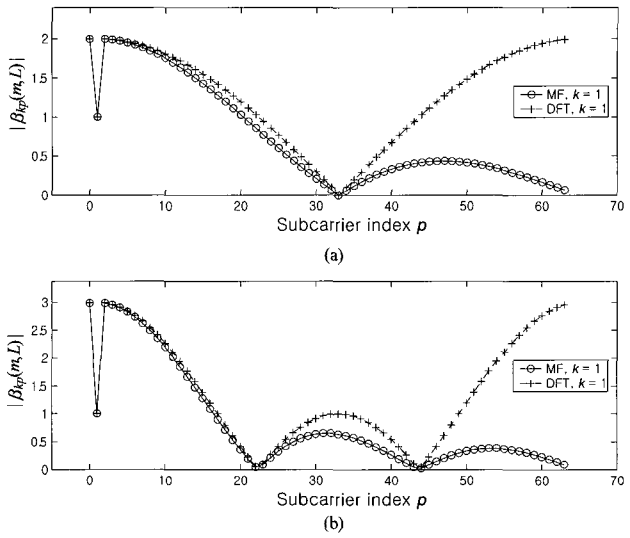

Fig. 1. Magnitude of the discrepancy factor $\beta_{kp}(m, L)$ for $k = 1$ and $L = 16$ when $L_c - 1 = 20$: (a) $m = 18$, (b) $m = 19$.

Table 1. Illustrative MF and DFT outputs: $L_c - 1 > L$.

de-OFDM input (i.e., ch. output)	Simulated outputs (MF & DFT)	Numerical outputs	
		MF	DFT
$0.04 - 0.21i$	$0.66 - 0.66i$	$0.96 - 1.03i$	$0.66 - 0.66i$
$-0.13 + 0.05i$	$-0.55 + 0.84i$	$-0.29 + 0.42i$	$-0.55 + 0.84i$
$0.13 - 0.05i$	$-0.34 - 0.66i$	$-0.15 - 1.10i$	$-0.34 - 0.66i$
$0.13 - 0.30i$	$0.87 - 0.16i$	$0.97 - 0.57i$	$0.87 - 0.16i$
$-0.13 - 0.20i$	$-0.34 + 0.34i$	$-0.31 + 0.02i$	$-0.34 + 0.34i$
$0.38 - 0.30i$	$0.16 - 0.87i$	$0.18 - 1.06i$	$0.16 - 0.87i$
$0.13 + 0.30i$	$-0.34 - 0.66i$	$-0.27 - 0.73i$	$-0.34 - 0.66i$
$0.13 + 0.05i$	$0.16 + 0.13i$	$0.35 + 0.14i$	$0.16 + 0.13i$

OFDM are randomly generated with its energy normalized to 1. For $L_c - 1 \leqslant L$, we have observed that the numerical data at the outputs of the MF and DFT with N samples/OFDM block as per the Nyquist rate are exactly the same both from simulation and numerical evaluation (not shown as well known). However, as shown in Table 1, with the same configuration except for the channel, i.e., $L_c - 1 > L$, there exists some discrepancy between simulated and numerically evaluated data. Two important observations can be made from this table: i) Simulated data for the MF- and DFT-based processing are the same and they agree with those of numerical evaluation from the DFT-based processing and ii) numerically evaluated data for the MF-based processing do not agree with those in i). Table 2 further shows that when more samples are used for the MF-based processing in simulation, the discrepancy between the simulated and numerically evaluated becomes less.

To illustrate the effect of the discrepancy and sampling rate on the OFDM demodulation, we look at the correlation between the k-th basis function from the first path and the basis functions from the other delayed paths of an N_p-path channel. For this purpose, the OFDM signals are generated as aforementioned but with $N = 64$, $L = 16$, and $T_b' = 4.0$ μs with all complex data $\{X_{n,k}\}$ set to 1. The MF processing is used to easily

Table 2. MF outputs for varied number of samples: $L_c - 1 > L$.

MF simulated outputs			Numerical outputs (MF)
N samples /block	$2N$ samples /block	$32N$ samples /block	
$0.66 - 0.66i$	$0.81 - 0.99i$	$0.95 - 1.03i$	$0.96 - 1.03i$
$-0.55 + 0.84i$	$-0.45 + 0.53i$	$-0.30 + 0.42i$	$-0.29 + 0.42i$
$-0.34 - 0.66i$	$-0.29 - 0.93i$	$-0.16 - 1.09i$	$-0.15 - 1.10i$
$0.87 - 0.16i$	$0.89 - 0.37i$	$0.96 - 0.56i$	$0.99 - 0.57i$
$-0.34 + 0.34i$	$-0.32 + 0.19i$	$-0.31 + 0.03i$	$-0.31 + 0.02i$
$0.16 - 0.87i$	$0.20 - 0.96i$	$0.18 - 1.06i$	$0.18 - 1.06i$
$-0.34 - 0.66i$	$-0.26 - 0.71i$	$-0.26 - 0.73i$	$-0.26 - 0.73i$
$0.16 + 0.13i$	$0.29 + 0.11i$	$0.35 + 0.14i$	$0.35 + 0.14i$

allow two different sampling rates, N and $2N$ per OFDM block. Fig. 2(a) shows that for the considered scenario of $N_p = 2$, the cross-correlation is very small when $m = 15$ as expected and its difference due to the sampling rates used is negligible, but when $m = 19$, the cross-correlation is dramatically larger than case (i) and the difference due to the sampling rates increases with the subcarrier index. A similar observation can be made in Fig. 2(b) where the correlation is calculated between the first-path k-th basis function and the sum of all other multipath components. It is clear, in addition to the well-known fact that the subcarrier orthogonality is destroyed in OFDM when the GI is insufficient, that this situation is worse in the N-point DFT-based processing than the MF-based or its somewhat practical discrete-time implementation with a sampling rate higher than N per OFDM block.

IV. ANALYSIS OF LINK PERFORMANCE

For the effect of the discrepancy on the link performance, we adopt the analysis in [8] performed in the notion of the DFT-based processing, but with some minor corrections[1] and further extend it for the MF-based processing. We assume $f_D T_b' \ll 1$, i.e., time-invariant over the OFDM block, for simplicity as we are mainly focused on the discrepancy. Note that while in the previous sections L is set to a preset value and $L_c - 1$ is varied, the analysis in [8] is presented with $L_c - 1$ set to a preset value and L varied from 0 to $L_c - 1$. In this section, we follow the way in [8] for easier referencing of our analysis to it. As part of this, $\lambda_{kp}(m)$, $\mu_{kp}(m)$, and $\beta_{kp}(m, L)$ are substituted by their full expressions and integrated in the final expressions. A key relationship for such comparison is

$$\frac{1}{N}\sum_{\ell=0}^{L_c-L-2}\sum_{m=\ell+L+1}^{L_c-1} c_m = \sum_{m\in\{m>L\}}\frac{m-L}{N}c_m \tag{14}$$

for $m > L$ and $L_c > L + 1$. From (8)–(13), the k-th OFDM demodulator output during the n-th block can be written as

$$Y_{n,k} = H_{kk}^{(n)} X_{n,k} + Z_{n,k} + S_{n,k} + N_{n,k} \tag{15}$$

where $H_{kk}^{(n)} X_{n,k}$ is the signal component, $Z_{n,k}$ is the ICI from the n-th block, $S_{n,k}$ is the ISI from the $(n-1)$-th block, and

[1]Based on numerical evaluation of (6) in [8], and (7) and (8) of this paper, which agree with the numerical results from [2] and [3], we believe that (6) in [8] is valid for $L \le L_c - 1$ but invalid for $L > L_c - 1$.

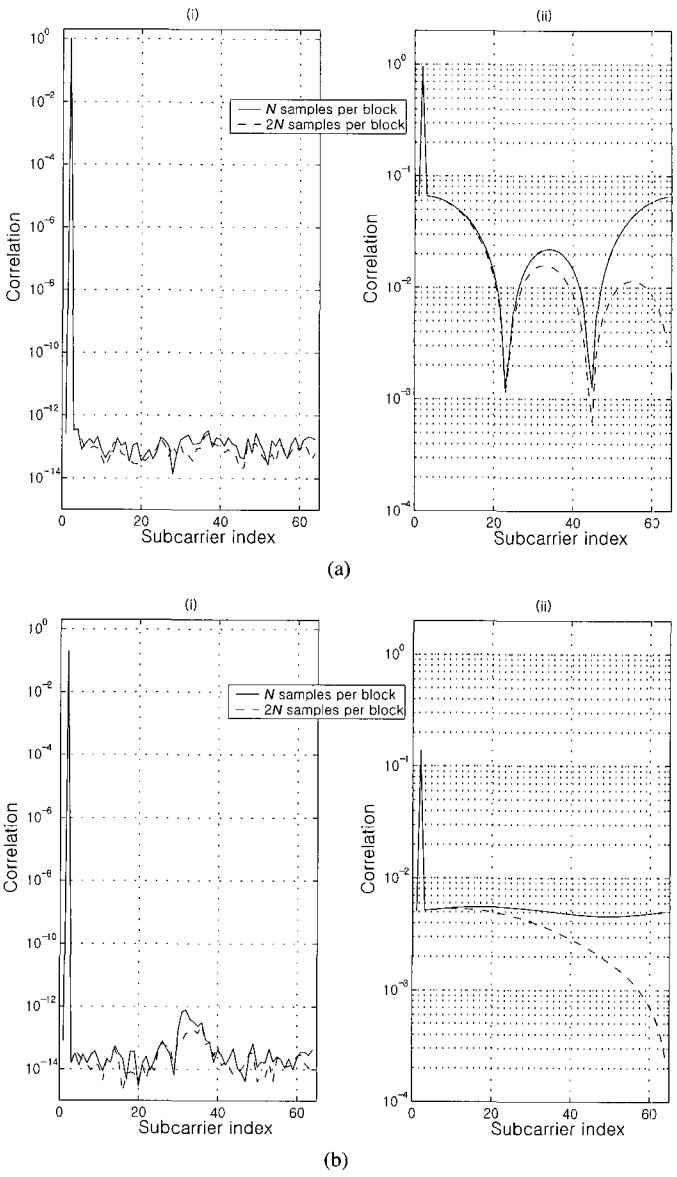

Fig. 2. Correlation between the first-path second subcarrier ($k = 1$) basis function and sum of all basis functions $\phi_k(t)$ from the other delayed paths: $N = 64$, $L = 16$, and $T_b' = 4\mu$s: (a) $N_p = 2$ with the 2nd path delay of (i) $m = 15 < L$ and (ii) $m = 19 > L$, (b) $N_p = L_c$ paths with (i) $L_c - 1 = 15 < L$ and (ii) $L_c - 1 = 19 > L$.

$N_{n,k}$ is the AWGN. The frequency-domain transfer function for the signal can be rewritten from (9) but with the use of summations in [8] as

$$H_{kk}^{(n)} = \frac{1}{N}\left[\sum_{\ell=\max(0,L_c-L-1)}^{N-1}\sum_{m=0}^{L_c-1} c_m e^{-j2\pi km/N} + \sum_{\ell=0}^{L_c-L-2}\sum_{m=0}^{\ell+L} c_m e^{-j2\pi km/N}\right] \tag{16}$$

and its variance $\sigma_H^2 = E\{H_{kk}^{(n)}(H_{kk}^{(n)})^*\}$ can be derived as

$$\sigma_H^2 = \frac{1}{N^2}\left[\sum_{\ell=\max(0,L_c-L-1)}^{N-1}\sum_{u=\max(0,L_c-L-1)}^{N-1}\sum_{m=0}^{L_c-1}\sigma_m^2 + 2\sum_{\ell=\max(0,L_c-L-1)}^{N-1}\sum_{u=0}^{L_c-L-2}\sum_{m=0}^{u+L}\sigma_m^2 + \sum_{\ell=0}^{L_c-L-2}\sum_{u=0}^{L_c-L-2}\sum_{m=0}^{\min(u,\ell)+L}\sigma_m^2\right] \quad (17)$$

where σ_m^2 is the power gain of the m-th multipath component. As they are different for the MF- and DFT-based processing, the second and third terms of (15) are separately discussed in the next subsections. The AWGN term in (15) can be written as $N_{n,k} = (1/\sqrt{N})\sum_{p=0}^{N-1} n_{n,k}e^{-j2\pi kp/N}$ such that its variance is given by $\sigma_N^2 = N_o$, where N_o is the one-sided power spectral density of the AWGN.

A. Interference in the DFT-Based Processing

The ICI term in (15) is from the other subcarriers in the current block and can be written as

$$Z_{n,k} = \frac{1}{N}\sum_{p\neq k} X_{n,p} \times \left[\sum_{\ell=\max(0,L_c-L-1)}^{N-1}\sum_{m=0}^{L_c-1} c_m e^{-j2\pi pm/N}e^{j2\pi\ell(p-k)/N} + \sum_{\ell=0}^{L_c-L-2}\sum_{m=0}^{\ell+L} c_m e^{-j2\pi pm/N}e^{j2\pi\ell(p-k)/N}\right] \quad (18)$$

and the ISI term is from the previous block and simplified to

$$S_{n,k} = \frac{1}{N}\sum_{p=0}^{N-1} X_{n-1,p}\sum_{\ell=0}^{L_c-L-2} \times \sum_{m=\ell+L+1}^{L_c-1} c_m e^{j2\pi p(L-m)/N}e^{j2\pi\ell(p-k)/N}. \quad (19)$$

Following the same approach as in [8], the variances of the ICI and ISI, i.e., $\sigma_Z^2 = E\{Z_{n,k}Z_{n,k}^*\}$ and $\sigma_S^2 = E\{S_{n,k}S_{n,k}^*\}$, respectively, can be written as

$$\sigma_Z^2 = \frac{E_s'}{N^2}\left[N(N-\max(0,L_c-L-1))\sum_{m=0}^{L_c-1}\sigma_m^2 + N\sum_{\ell=0}^{L_c-L-2}\sum_{m=0}^{\ell+L}\sigma_m^2 - \sum_{\ell=\max(0,L_c-L-1)}^{N-1}\sum_{u=\max(0,L_c-L-1)}^{N-1}\sum_{m=0}^{L_c-1}\sigma_m^2 - 2\sum_{u=\max(0,L_c-L-1)}^{N-1}\sum_{\ell=0}^{L_c-L-2}\sum_{m=0}^{\ell+L}\sigma_m^2 - \sum_{\ell=0}^{L_c-L-2}\sum_{u=0}^{L_c-L-2}\sum_{m=0}^{\min(u,\ell)+L}\sigma_m^2\right] \quad (20)$$

where $E_s' = E_s/(1+L/N)$ is the effective symbol energy with E_s denoting the symbol energy of i.i.d. zero mean data $\{X_{n,k}\}$ and

$$\sigma_S^2 = \frac{E_s'}{N}\sum_{\ell=0}^{L_c-L-2}\sum_{m=\ell+L+1}^{L_c-1}\sigma_m^2. \quad (21)$$

B. Interference in the MF-Based Processing

Extending the results in Section IV-A with the discrepancy factor in (13), the ICI and ISI terms in (15) in this case are derived as

$$Z_{n,k} = -\frac{1}{N}\sum_{p\neq k} X_{n,p}\sum_{\ell=0}^{L_c-L-2}\sum_{m=\ell+L+1}^{L_c-1} c_m e^{-j2\pi pm/N} \times e^{j\pi(p-k)(m-L)/N}\operatorname{sinc}\left(\frac{\pi(p-k)(m-L)}{N}\right) \quad (22)$$

$$S_{n,k} = \frac{1}{N}\sum_{p=0}^{N-1} X_{n-1,p}\sum_{\ell=0}^{L_c-L-2}\sum_{m=\ell+L+1}^{L_c-1} c_m e^{j2\pi p(L-m)/N} \times e^{j\pi(p-k)(m-L)/N}\operatorname{sinc}\left(\frac{\pi(p-k)(m-L)}{N}\right). \quad (23)$$

Then, the variances of $Z_{n,k}$ and $S_{n,k}$ can be written as

$$\sigma_Z^2 = \frac{E_s'}{N^2}\left[\frac{1}{N}\left(\sum_{k=0}^{N-1}\sum_{p=0}^{N-1}\left|\sum_{\ell=0}^{L_c-L-2}\sum_{m=\ell+L+1}^{L_c-1} c_m e^{-j2\pi pm/N} \times e^{j\pi(p-k)(m-L)/N}\operatorname{sinc}\left(\frac{\pi(p-l)(m-L)}{N}\right)\right|^2 - \sum_{p=0}^{N-1}\left|\sum_{\ell=0}^{L_c-L-2}\sum_{m=\ell+L+1}^{L_c-1} c_m e^{-j2\pi pm/N}\right|^2\right)\right] \quad (24)$$

$$\sigma_S^2 = \frac{E_s'}{N^2}\left[\frac{1}{N}\sum_{k=0}^{N-1}\sum_{p=0}^{N-1}\left|\sum_{\ell=0}^{L_c-L-2}\sum_{m=\ell+L+1}^{L_c-1} c_m e^{j2\pi p(L-m)/N} \times e^{j\pi(p-k)(m-L)/N}\operatorname{sinc}\left(\frac{\pi(p-l)(m-L)}{N}\right)\right|^2\right]. \quad (25)$$

C. Error Rates

With the variances from the previous subsections, the average SINR can be written as [8]

$$\bar{\gamma} = E_s'\sigma_H^2/(\sigma_Z^2+\sigma_S^2+N_o) \quad (26)$$

where the interference terms in the denominator already include the effective symbol energy E_s'. Then, considering the Gray-mapped 16-QAM OFDM system, one can write the BER averaged over Rayleigh fading as [8]

$$P_{b,Q} = \frac{3}{8}\left(1-\sqrt{\frac{\bar{\gamma}}{\bar{\gamma}+10}}\right) + \frac{1}{4}\left(1-\sqrt{\frac{9\bar{\gamma}}{9\bar{\gamma}+10}}\right) - \frac{1}{8}\left(1-\sqrt{\frac{5\bar{\gamma}}{5\bar{\gamma}+2}}\right). \quad (27)$$

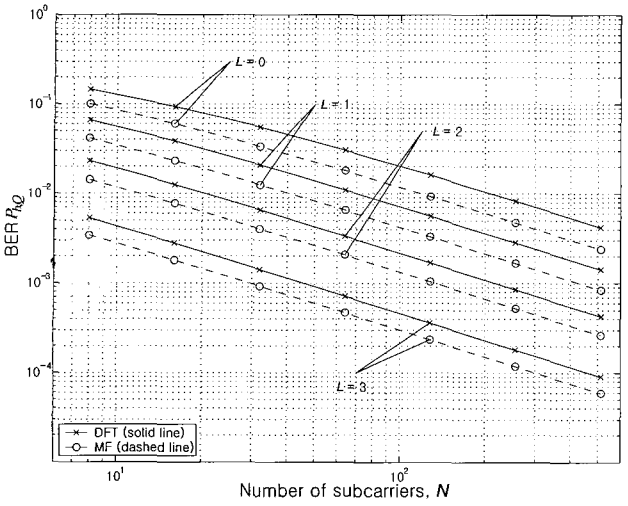

(a)

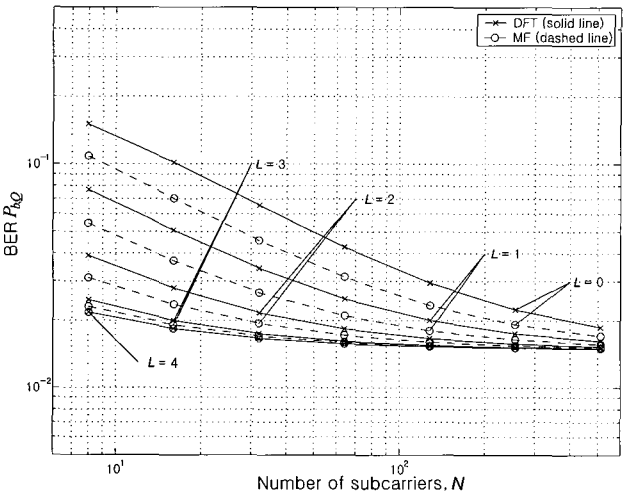

(b)

Fig. 3. BER vs. $N = \{8, 16, 32, 64, 128, 256, 512\}$ when $L_c = 5$ and $L = \{0, 1, 2, 3, 4\}$. In (a), the BER values when $L = 4 = L_c - 1$ are all zero (not shown): (a) $E_b/N_o = \infty$, (b) $E_b/N_o = 15$ dB.

D. Numerical Results

For the accuracy of the expressions for the DFT-based, i.e., (16), (18), and (19), and those for the MF-based processing, i.e., (16), (22), and (23), we have verified by numerical evaluation (not shown) that they produce the same results under all scenarios in Section III-C, e.g., Table 1. Below, the discrepancy in link performance between the MF- and DFT-based processing is evaluated in terms of BER given by (27) for various situations and $L_c = 5$. The BERs of both MF-based and DFT-based are shown in Fig. 3(a) as a function of the number of subcarriers N for varying GI lengths L without the presence of noise, i.e., $E_b/N_o = \infty$. Note that the BER difference exists between the MF-/DFT-based processing and becomes slightly larger as L becomes shorter. Also, we can observe that as L becomes shorter and thus, effectively the maximum channel delay exceeds the GI, the BERs decrease as expected. On the other hand, the BER

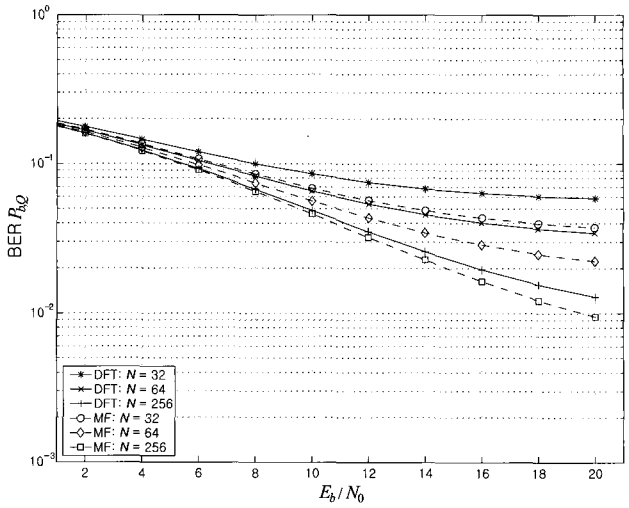

Fig. 4. BER vs. E_b/N_o when $L_c = 5$ and $L = 0$.

is improved with a larger N as it means a longer effective duration of OFDM for the same fundamental period T and thus less ISI.

From Fig. 3(b) for $E_b/N_o = 15$ dB, the same observations can be made except that a noise floor is observed at a BER of about 1.4×10^{-2}. That is, for a given E_b/N_o, the BER performance reaches a limit and cannot be further improved by increasing N in practice, and the performance discrepancy between the MF-/DFT-based processing can be considered effectively disappeared. Fig. 4 shows the BERs as a function of E_b/N_o for the case of no guard interval, i.e., $L = 0$. Note that as the E_b/N_o increases, the performance difference between the MF-/DFT-based processing becomes larger.

V. CONCLUSIONS

We have shown that there exists inherent discrepancy in the amount of ISI/ ICI and thus link performance between the MF- and DFT-based processing for an OFDM system in excessively dispersive multipath channels. Also, the numerical results in this paper suggest that there could be a discrete-time implementation of an OFDM receiver more robust in harsh multipath environment than the typical N-point DFT.

REFERENCES

[1] S. B. Weinstein and P. M. Ebert, "Data transmission by frequency-division multiplexing using the discrete Fourier transform," *IEEE Trans. Commun. Technol.*, vol. COM-19, no. 5, pp. 628–634, Oct. 1971.

[2] E. Viterbo and K. Fazel, "How to combat long echoes in OFDM transmission schemes: Sub-channel equalization or more powerful channel coding," in *Proc. IEEE GLOBECOM'95*, Nov. 1995, pp. 2069–2074.

[3] S. Trautmann, T. Karp, and N. J. Fliege, "Frequency domain equalization of DMT/OFDM systems with insufficient guard interval," in *Proc. IEEE ICC 2002*, 28 Apr.–2 May 2002, pp. 1646–1650.

[4] J. L. Seoane, S. K. Wilson, and S. Gelfand, "Analysis of intertone and interblock interference in OFDM when the length of the cyclic prefix is shorter than the length of the impulse response of the channel," in *Proc. IEEE GLOBECOM'97*, Nov. 1997, pp. 32–36.

[5] K. V. Acker, G. Leus, M. Moonen, O. van de Wiel, and T. Pollet, "Per tone equalization for DMT-based systems," *IEEE Trans. Commun.*, vol. 49, no. 1, pp. 109–119, Jan. 2001.

[6] R. Morrison, L. J. Cimini Jr., S. K. Wilson, "On the use of a cyclic extension in OFDM," in *Proc. IEEE VTC 2001-fall*, Oct. 2001, pp. 664–668.
[7] K. Sathananthan and C. Tellambura, "Probability of error calculation of OFDM systems with frequency offset," *IEEE Trans. Commun.*, vol. 49, no. 11, pp. 1884–1888, Nov. 2001.
[8] Y. H. Kim, I. Song, H. G. Kim, T. Chang, and H. M. Kim, "Performance analysis of a coded OFDM system in time-varying multipath Rayleigh fading channels," *IEEE Trans. Veh. Technol.*, vol. 48, no. 5, pp. 1610–1615, Sept. 1999.
[9] G. D. Pantos, A. G. Kanatas, and P. Constantinou, "Performance evaluation of OFDM transmission over a challenging urban propagation environment," *IEEE Trans. Broadcast.*, vol. 49, no. 1, pp. 87–96, Mar. 2003.

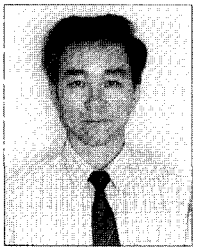

Wookwon Lee received the B.S. degree in electronic engineering from the Inha University, Korea, in 1985, and the M.S. and D.Sc. degrees in electrical engineering from the George Washington University, Washington DC, in 1992 and 1995, respectively. He is currently on the faculty of the Department of Electrical Engineering at the University of Arkansas, Fayetteville, Arkansas. Prior to this, he was with Samsung Electronics in Korea, Bell Atlantic in Arlington, VA, U.S.A., and Nortel Networks in Ottawa, ON, Canada. His current research interests include cooperative communications, hybrid RF/optical wireless communications, and design of disaster-resilient wireless communication systems.

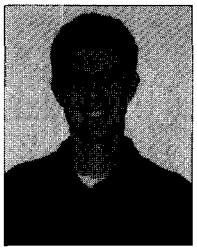

Christopher S. Curry received the B.S. and M.S. degrees in electrical engineering from the University of Arkansas in 2004 and 2005, respectively. He is currently an RF engineer with Raytheon Company in Dallas, TX. His research interests include OFDM-based wireless systems, adaptive signal processing, and ultra-wideband communication systems.